AN INSTITIÚID UM THAIGHDE EACNAMAÍOCHTA AGUS SÓISIALTA
ESRI ECONOMIC & SOCIAL RESEARCH INSTITUTE

Developing data-driven damage and adaptation functions for Integrated Assessment Models: An application in AD-MERGE 2.0

Kelly de Bruin, Kirsten Everett, Daniel Cassidy

ESRI Working Paper No. 838

July 2026

Developing data-driven damage and adaptation functions for Integrated Assessment Models: An application in AD-MERGE 2.0

Kelly de Bruin, Kirsten Everett and Daniel Cassidy

July 2026

Abstract

Integrated Assessment Models (IAMs) have been the primary tool for studying the global trade-offs of climate change mitigation over the past decades. These models rely on estimated functions of climate change induced economic damages. These are, however, based on severely limited or decades-old data, or both. This paper aims to estimate the most robust possible regional impact cost functions given the available data and implement them into the AD-MERGE 2.0 IAM. We estimate the impacts of climate change on coastal flooding, river flooding, mortality and morbidity, energy consumption, labour productivity and tourism using recent observational data or results of recent modelling exercises. In addition, we estimate proactive and reactive adaptation benefits, as well as associated adaptation costs. The resulting global damage function aligns closely with the estimated damage functions reported in Howard and Sterner (2017) and extends the observed pattern, whereby more recent damage functions imply greater damage for given temperature increases. Regional disparities in the damage function are substantial, with Africa and the Other Asian States incurring greater damage for each incremental increase in temperature than other regions.

JEL codes: Q54, Q40
Keywords: Damage functions, IAM, Climate change

1 Introduction

Estimating the economic impacts of climate change has long been a central focus of the climate economics literature; however, bottom-up damage function estimates depend on both economic and non-economic data that change significantly over time (van der Wijst et al., 2023). Consequently, these damage functions require periodic revision using more recent data and methodologies, or they risk becoming outdated (Auffhammer, 2018). This is a concern given that these damage functions are embedded in Integrated Assessment Models (IAMs), which form an important methodological tool to investigate the global trade-offs of mitigation (Van Vuuren et al., 2011). If IAMs informing policy formulation are reliant on outdated and imprecise estimates, this may have substantial implications, particularly where more recent evidence suggests larger projected damages than previously reported and hence higher levels of recommended mitigation.

This paper aims to estimate damage functions as robustly as possible for application in IAMs. We calibrate damage functions to implement into AD-MERGE 2.0 covering the fifteen regions of the model using recent data across six impact categories: coastal flooding, river flooding, mortality and morbidity, energy consumption, labour productivity and tourism. Coastal flooding damages are assessed as a function of sea-level rise, while the remaining impacts are estimated with respect to changes in temperature. Both proactive (stock) and reactive (flow) adaptation costs and benefits are quantified. The updated damage functions and adaptation estimates are intended for use in revisions to macroeconomic climate models, particularly Integrated Assessment Models such as the AD-MERGE 2.0 model (Amirmoeini et al., 2026), which inform policymakers. The damage functions in this paper are generally based on country-level data but aggregated to the AD-MERGE 2.0 regions. This model is an updated version of the AD-MERGE 1.0 model (Bahn, Bruin, & Fertel, 2019), which in turn is based on the MERGE model (Manne, Mendelsohn, & Richels, 1995). AD-MERGE 2.0 differs from the previous version in that it includes hydrogen, updates the energy modelling components, increases the regional representation to 15 regions and contains recalibrated damage and adaptation functions. This model can be used to understand the trade-offs of new mitigation technologies, impacts and adaptation, focusing on regional differences (Amirmoeini et al., 2026).

The analysis in this paper integrates a range of impact-specific datasets drawn from established empirical sources. Coastal flooding damages are estimated using the CIAM model (Diaz, 2016), with river flooding impacts derived from the Aqueduct Flooding database, which is based on the GLOFRIS model (Ward et al., 2020; Winsemius et al., 2013; World Resources Institute, 2020). Health impacts, measured through mortality and morbidity, are based on data from the Institute for Health Metrics and Evaluation (2024) and World Health Organisation (2014). Energy consumption and labour productivity impacts are constructed using data from the Austalian Bureau of Statistics (2024), Ezrati (2023), International Labour Organisation (2024), Stats NZ (2025) and Climate Impact Lab and UNDP's Human Development Report Office (2022). Tourist arrivals are estimated using the Hamilton et al. (2005) framework, as implemented in de Bruin and Ayuba (2020), using data from the CIA (2024), Our World in Data (n.d.) and The World Bank (2024). The resulting impact estimates are aggregated at the regional level and used to calibrate the damage function parameters for each region. A detailed account of the estimation procedures for each impact category, region, and Representative Concentration Pathways (RCP) scenario (Van Vuuren et al., 2011) is provided in section 2. Adaptation costs and benefits are also estimated for each impact category based on the relevant data and literature.

In the literature, damage functions have been estimated using evidence from either individual studies or meta-analyses of the existing literature (Howard & Sterner, 2017; Tol, 2002a, 2002b), whereas other studies calibrate them through direct estimation using underlying empirical data (Roson & Sartori, 2016). A common criticism of some Integrated Assessment Models is the limited geographical coverage underlying their damage estimates (Diaz & Moore, 2017). This paper addresses this limitation by calibrating regional damage functions using the latest available publicly accessible datasets, where applicable, spanning a broad range of countries and regions.

The results indicate that the global damage function estimated in this paper expressed as a share of GDP increases more sharply with temperature than in earlier studies such as Tol (2014, 2009) and Nordhaus (2013). Regional differences are substantial, with Africa and the Other Asian States exhibiting considerably higher damages as a percentage of GDP for each incremental increase in temperature relative to other regions

This paper presents updated damage functions and adaptation estimates that can be incorporated into Integrated Assessment Models. To facilitate replication and further research, the underlying data sources and methodological procedures are documented in detail. By calibrating damage functions using contemporary, country-level data, the analysis supports the development of climate impact assessments that provide policymakers with more realistic insights. Nevertheless, the study does not undertake a formal uncertainty analysis, and the accuracy of the estimated damage functions remains contingent on the quality of the underlying data. The remainder of the paper is organised as follows. Section 2 reviews the literature for each climate change impact category, outlines the methodology, and presents the corresponding results. Section 3 describes the calibration of regional damage functions. Section 4 details the estimation of adaptation costs and residual damages, and Section 5 concludes.

2 Impact categories

Climate change gives rise to both physical and socioeconomic impacts that translate into economic damages. Empirical studies link temperature changes to tourism demand, mortality and morbidity, labour productivity and energy consumption (Baccini et al., 2008; Deschênes & Greenstone, 2011; Sahu, Sett, & Kjellstrom, 2013; Schleypen et al., 2019; Yu, Schwartz, & Walsh, 2009). Climatic changes also influence the frequency, intensity, duration and spatial distribution of river flooding, generating economic damage at both regional and global scales (Abatzoglou & Williams, 2016; Dottori et al., 2018; IPCC, 2012; Narita, Tol, & Anthoff, 2009, 2010; Seneviratne et al., 2021; Winsemius et al., 2016). Damage functions are used in Integrated Assessment Models (IAMs), such as DICE (Nordhaus, 1992), RICE (Nordhaus & Yang, 1996), FUND (Tol, 2002a, 2002b), WITCH (Bosetti, Carraro, Galeotti, Massetti, & Tavoni, 2006) and MERGE (Manne et al., 1995), to convert physical and socioeconomic impacts of climate change into economic damages. Existing damage functions, including those developed by Tol (2002a, 2002b) and Roson and Sartori (2016), are largely based on estimates drawn from non-economic impact studies. Whilst many IAMs before 2009 mainly included adaptation implicitly (i.e. through assumptions), adaptation has since explicitly been incorporated into DICE in the AD-DICE model (de Bruin, Dellink, & Tol, 2009a), RICE in the AD-RICE model (de Bruin, 2014; de Bruin, Dellink, & Tol, 2009b) and the FEEM-RICE model (Bosello, 2010), WITCH in the AD-WITCH model (Bosello, Carraro, & De Cian, 2010) and MERGE in the AD-MERGE model (Amirmoeini et al., 2026; Bahn et al., 2019).

This paper contributes to the literature by incorporating updated data-driven damage functions and adaptation in the AD-MERGE 2.0 model. The damage functions in this paper are based on data from six impact categories: sea level rise, river flooding, human health, energy consumption, labour productivity and tourism. The rest of the paper explains how these damages are estimated and details the calibration process for adaptation.

2.1 Sea level rise

Sea level rise is a well-established consequence of climate change, although its projected magnitude depends on climate scenarios, regional characteristics, and assumed levels of adaptation (Depsky et al., 2023; Diaz, 2016; Wong et al., 2014). Rising sea levels increase the risk of coastal flooding, with adverse impacts on coastal ecosystems, economic activity, and residential areas (Wong et al., 2014). Damage estimates are sensitive to assumptions about population, socioeconomic conditions, the magnitude of sea level rise, regional exposure, and adaptation strategies (Depsky et al., 2023; Diaz, 2016; Hinkel et al., 2013). Consequently, estimated damages differ across modelling frameworks, including DIVA, CIAM or DSCIM-Coastal (Depsky et al., 2023; Diaz, 2016; Hinkel, 2005; Hinkel & Klein, 2009). Despite these differences, the models consistently indicate that adaptation reduces damage and that its benefits exceed its costs tenfold (Depsky et al., 2023; Diaz, 2016; Hinkel et al., 2013).

2.1.1 Methodology

This paper draws on damage estimates from the CIAM model developed by Diaz (2016), which estimates the monetary value of damages from coastal flooding arising from sea level rise and storm surges under RCP2.6, RCP4.5 and RCP8.5. CIAM divides the global coastline into approximately 12,000 segments and, within each segment, determines the least-cost adaptation strategy to minimise expected flood damages (Diaz, 2016). Flood damages for each region (r), RCP and time petiod (t), denoted $GD_{r,t,RCP,flood}$ are represented as the sum of inundation costs ($InundationCost$), wetland loss ($WetlandCost$), relocation loss ($RelocationCost$) and capital losses and population impacts from storm events ($StormCost$). All damage components are reported in constant 2010 US dollars, with aggregate damages used for the analysis.

This model is run for each coastal segment to estimate coastal-flooding damage under both no-adaptation and adaptation for each RCP. The results at coastal segment level are then aggregated to the AD-MERGE 2.0 regions (see Appendix A.5 for the country composition of each region).

$$GD_{r,t,RCP,flood} = InundationCost_{r,t,RCP} + WetlandCost_{r,t,RCP} + RelocationCost_{r,t,RCP} + StormCost_{r,t,RCP} \tag{1}$$

Damage estimates are converted from constant 2010 to constant 2015 US dollars, in line with the AD-MERGE 2.0 base year, assuming a three per cent annual inflation rate, and are expressed as a percentage of GDP.

2.1.2 Estimates

Table 1 reports coastal flooding damages as a percentage of GDP by region and RCP for 2050 and 2100. Median sea level rise under RCP4.5 is projected to reach 0.26 m by 2050 and 0.59 m by 2100, while under RCP8.5 median sea level rise is projected to reach 0.29 m and 0.79 m, respectively (Diaz, 2016).

Table 1: Projected coastal flooding damages (% of GDP)

	2050		2100	
Region	RCP4.5	RCP8.5	RCP4.5	RCP8.5
Africa (AFR)	3.63	6.18	0.85	13.03
Australia and New Zealand (ANZ)	1.60	2.50	1.06	3.82
Brazil (BRA)	0.76	1.27	0.43	2.46
Canada (CAN)	0.00	0.00	0.00	0.00
China (CHN)	0.64	0.82	0.58	1.13
Central and Latin America (CLA)	4.21	5.96	1.74	8.22
India (IND)	0.10	0.18	0.10	0.64
Japan and South Korea (JSK)	0.36	0.48	0.41	0.60
Middle East (MEA)	1.95	2.99	1.05	3.37
Mexico (MEX)	0.21	0.32	0.15	0.63
Other Asia (OAS)	6.80	9.34	2.88	12.53
Other Eurasia (OEA)	0.24	0.32	0.20	0.52
Russia (RUS)	0.07	0.11	0.04	0.18
United States of America (USA)	1.03	1.21	0.94	1.75
Western Europe (WEUR)	2.30	2.85	1.58	3.32

Source: Authors' compilation using the CIAM model (Diaz, 2016).

In 2050, the regions with the largest annual damage as a percentage of their GDP in RCP 4.5 and RCP 8.5, respectively, are OAS (6.8 per cent and 9.3 per cent), CLA (4.2 per cent and 5.96 per cent) and Africa (3.6 per cent and 6.2 per cent). These regions have extensive coastlines and relatively low GDP levels compared with other areas. When coastal flooding causes significant damage through wetland loss, storm damage, inundation, and relocation across many coastal segments, the aggregate impact is substantial relative to GDP. These effects only increase in 2100 under RCP8.5. However, in 2100 for RCP4.5, for most regions it looks as if the annual coastal flooding damage as a percentage of GDP is decreasing. This reflects the fact that, although absolute damages continue to rise, GDP growth exceeds the increase in damages, resulting in a lower damage-to-GDP ratio relative to 2050.

2.2 River flooding

Existing studies indicate that climate change alters river flood risk unevenly across countries and regions, with some experiencing increased flood risk and others facing reductions (Arnell & Gosling, 2016). Changes in flood risk affect estimated annual river flood damages and lead to cross-country variation in river flooding damages as a share of GDP (World Resources Institute, 2020).

Despite this heterogeneity, the overall evidence indicates an increase in river flooding and associated economic damage under climate change. The extent of projected increases varies across climate scenarios, adaptation assumptions, and modelling frameworks (Dottori et al., 2018; Lincke et al., 2018; Winsemius et al., 2016).

2.2.1 Methodology

The Aqueduct Floods database provides estimates of expected annual river flood damages expressed as a percentage of GDP across countries and climate scenarios (Ward et al., 2020; World Resources Institute, 2020). These estimates were derived by Ward et al. (2020) using the Global Flood Risk with IMAGE Scenarios (GLOFRIS) model (Winsemius et al., 2013). Ward et al. (2020) simulate river flooding under a baseline and three climate change scenarios: RCP4.5 (SSP2), RCP8.5 (SSP2) and RCP8.5 (SSP3). Expected annual damages are calculated at the grid-cell level as the expected loss to GDP in locations where river flood levels exceed flood protection levels provided by existing dykes (Ward et al., 2020). The damage calculations account for flood events that are expected to occur at different frequencies, such as a one-in-100-year river flood.

For this analysis, country-level estimates of expected annual affected GDP and total GDP were extracted from the Aqueduct Floods database for each scenario (World Resources Institute, 2020). Countries were then mapped to their corresponding AD-MERGE 2.0 regions (see Appendix A.5), and both affected GDP and total GDP were aggregated from country to regional level. Regional river flood damages were subsequently calculated as the ratio of expected annual affected GDP to total GDP.

2.2.2 Estimates

The regional annual affected GDP, as a percentage of total GDP, is shown in Table 2 below for 2030 and 2050. The regions with the highest river flooding damage as a percentage of GDP are Other Asia (OAS), the Middle East (MEA), India (IND), and Africa (AFR). These effects are larger in the RCP8.5 scenario than the RCP4.5 scenario but over time they either increase or decrease. The latter is due to the rate of increase in damages compared to the rate of increase in regional GDP. When the increase in damages is not as steep as the increase in total GDP, the damages as a percentage of GDP may fall.

Table 2: Expected annual affected GDP as a share of GDP (%)

	2030		2050	
Region	RCP4.5	RCP8.5	RCP4.5	RCP8.5
Africa (AFR)	1.03	1.32	1.44	1.53
Australia and New Zealand (ANZ)	0.26	0.31	0.25	0.31
Brazil (BRA)	0.19	0.23	0.25	0.34
Canada (CAN)	0.48	0.72	0.62	0.65
China (CHN)	0.35	0.29	0.35	0.49
Central and Latin America (CLA)	0.40	0.51	0.51	0.69
India (IND)	1.50	1.91	1.79	2.53
Japan and South Korea (JSK)	0.17	0.32	0.20	0.35
Middle East (MEA)	1.11	2.21	1.41	1.61
Mexico (MEX)	0.14	0.17	0.18	0.22
Other Asia (OAS)	2.04	2.36	2.53	3.26
Other Eurasia (OEA)	0.20	0.15	0.23	0.15
Russia (RUS)	0.12	0.25	0.11	0.23
United States of America (USA)	0.08	0.13	0.09	0.12
Western Europe (WEUR)	0.13	0.86	0.13	0.92

Source: Authors' compilation using the Aqueduct Floods data (Ward et al., 2020; World Resources Institute, 2020).

River flooding damages as a percentage of GDP are lower than coastal flooding damages under RCP4.5 in 2050 for Africa (1.4 per cent compared with 3.6 per cent), OAS (2.5 per cent compared with 6.8 per cent) and MEA (1.4 per cent compared with 1.9 per cent). In contrast, for India, river flooding damages (1.8 per cent) exceed coastal flooding damages (0.1 per cent) under RCP4.5 in 2050. This highlights substantial geographic variation in the relative importance of coastal and river flooding impacts across regions. These differences have implications for the prioritisation of climate adaptation and risk-management policies, although information on adaptation measures, discussed in Section 4, is also required to inform policy decisions.

2.3 Human health

Climate-induced temperature changes can lead to significant mortality and morbidity impacts through heat exposure, dengue, malaria, diarrhoea and undernutrition. Temperature increases beyond a threshold value were found to increase heat-related mortality and morbidity, commonly measured using disability-adjusted life years (DALYs) (Baccini et al., 2008; Breitner et al., 2014; Deschênes, 2022; Deschênes & Greenstone, 2011; Song et al., 2021; World Health Organisation, 2014). Elderly cohorts of the population and children are found to be particularly vulnerable to heat-related mortality relative to adult cohorts (Baccini et al., 2008; Breitner et al., 2014; Chapman et al., 2022; Deschênes & Greenstone, 2011). Children were found to be particularly affected by climate-induced undernutrition (Grace, Davenport, Funk, & Lerner, 2012; Skoufias & Vinha, 2013).

Changes in precipitation patterns can also affect access to clean water, affecting the incidence of diarrhoeal cases. However, empirical studies report mixed evidence on the relationship between precipitation, temperature increases, and diarrhoeal incidence, with effects varying by season, diarrhoea type, location and the specific indicators used for temperature and precipitation (Bandyopadhyay et al., 2012; Carlton et al., 2016; Chou et al., 2010; Lloyd et al., 2007). Furthermore, climate-driven changes in temperature and rainfall may threaten food production in some regions, increasing the risk of undernutrition (Lloyd et al., 2011; Nelson et al., 2009; World Health Organisation, 2014). The magnitude of projected undernutrition impacts differs across regions and demographic groups and depends on modelling assumptions, including whether carbon dioxide fertilisation effects are incorporated and how undernutrition is measured (Dickerson et al., 2021; Lloyd et al., 2011; Nelson et al., 2009).

Climate-driven increases in temperature and rainfall can broaden the geographic range of mosquitoes, increasing the incidence of malaria and dengue (Dickerson et al., 2021; Liu-Helmersson et al., 2014; Mordecai et al., 2020; Rogers & Randolph, 2000; World Health Organisation, 2014). However, the effect of the increase in temperature and rainfall may be limited by existing temperature, rainfall and humidity factors, thus some regions may see a reduction in malaria cases (Caminade et al., 2014; Dickerson et al., 2021; Liu-Helmersson et al., 2014; Mordecai et al., 2020; Rogers & Randolph, 2000). Temperature increases below the peak temperature were associated with increased dengue infections and the growth rate of these infections (Liu-Helmersson et al., 2014; Siraj et al., 2017).

2.3.1 Methodology

The Institute for Health Metrics and Evaluation (2024) publishes the Global Burden of Disease dataset, which provides country-level estimates of deaths and years of life lost across a wide range of diseases. This paper focuses on dengue, diarrhoeal diseases, malaria, and nutritional deficiencies. Country-level data for these outcomes are aggregated to the AD-MERGE 2.0 regions for the 2015 base year and are reported in Figure 1.

Figure 1 indicates that India, Africa, and OAS record the highest numbers of deaths from diarrhoeal diseases, malaria, and nutritional deficiencies. Dengue-related deaths are also relatively high in India and OAS relative to other regions. Although ANZ, CAN and RUS appear to record zero deaths, this applies only to dengue and malaria. Deaths from diarrhoeal diseases and nutritional deficiencies do occur in these regions but are small relative to others and therefore not visible at the scale of the figure. While these figures represent total disease-related deaths in the base year, the analysis requires estimates of future mortality attributable to climate change, including both disease-related and heat-related mortality. To derive these estimates, data from the World Health Organisation (2014) are used.

The World Health Organisation (2014) provides estimates of additional mortality attributable to climate change for malaria, dengue, diarrhoeal disease (children under 15 years), undernutrition (children under five years), and heat exposure (adults aged 65 years and older). These estimates are for 2030 and 2050 under the A1b SRES emissions scenario. The WHO regions are mapped to the AD-MERGE 2.0 regions, and additional deaths are aggregated accordingly for each region and year. These values form the basis for the estimated climate-attributable mortality used in this paper. In addition to mortality counts, years of life lost (YLL) are also considered. Climate-attributable years of life lost (YLL_{CC}) are estimated by scaling baseline years of life lost from the Global Burden of Disease dataset for 2015 (YLL_{GBD}) (Institute for Health Metrics and Evaluation, 2024). The scaling factor is the ratio of deaths attributable to climate change reported by the World Health Organisation (2014) (PD_{WHO}) to total deaths from these causes in the Global Burden of Disease data (PD_{GBD}) (Institute for Health Metrics and Evaluation, 2024).

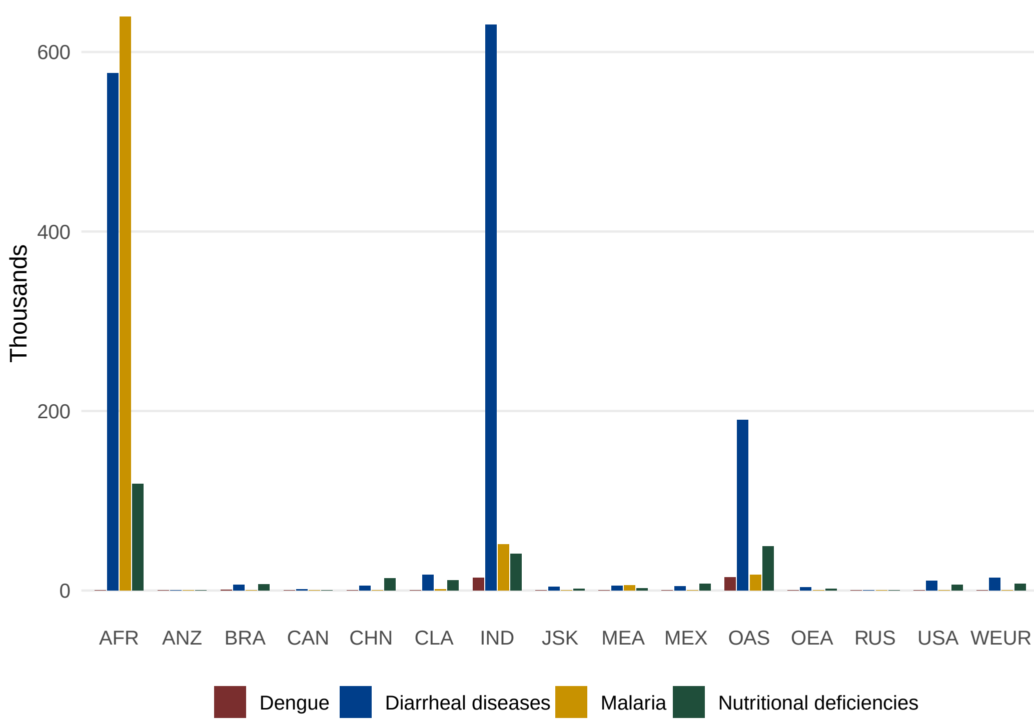

Figure 1: Global Burden of Disease death data for 2015 by region

Source: This was calculated based on Institute for Health Metrics and Evaluation (2024) data

$$YLL_{CC_{r,t}} = YLL_{GBD_{r,t}} \cdot \frac{PD_{WHO_{r,t}}}{PD_{GBD_{r,t}}} \tag{2}$$

Having estimated climate-attributable mortality and years of life lost, the associated economic costs are then calculated. GDP per capita is first computed for each region. Gross damages from climate-related mortality are subsequently estimated by multiplying the number of climate-attributable deaths in each region by regional GDP per capita and a valuation factor of 200 based on Cline (1992). This factor has been used in the literature (de Bruin & Ayuba, 2020; Tol, 2002a). Gross damages (GD), are calculated for each region (r) and time period (t) based on population deaths (PD), as shown in Equation 3.

$$GD_{r,t,PD} = PD_{WHO_{r,t}} \cdot 200 \cdot \frac{GDP_{r,t}}{Pop_{r,t}} \tag{3}$$

Gross damages from years of life lost are calculated for each region and time period by valuing climate-attributable years of life lost (YLL_{CC}) using regional GDP per capita and a valuation factor of 0.8. This valuation factor is based on the income elasticity from the value of statistical life (VSL) approach (OECD, 2012). Other IAM literature has used this valuation factor for morbidity (de Bruin & Ayuba, 2020; Link & Tol, 2006).

$$GD_{r,t,YLL} = YLL_{CC_{r,t}} \cdot 0.8 \cdot \frac{GDP_{r,t}}{Pop_{r,t}} \tag{4}$$

Finally, gross damages from all health impact channels are aggregated and divided by regional GDP to obtain total health damages expressed as a percentage of regional GDP.

2.3.2 Estimates

Table 3 reports climate change related deaths in 2030 and 2050, based on estimates from the World Health Organisation (2014) and aggregated to the AD-MERGE 2.0 regions.

Table 3: Annual climate-change-attributable deaths by region

Region	2030	2050
Africa (AFR)	159,915	123,056
Australia and New Zealand (ANZ)	93	236
Brazil (BRA)	858	2,032
Canada (CAN)	157	321
China (CHN)	9,420	18,685
Central and Latin America (CLA)	2,290	3,980
India (IND)	46,810	58,431
Japan and South Korea (JSK)	1,489	2,505
Middle East (MEA)	2,468	4,362
Mexico (MEX)	935	1,757
Other Asia (OAS)	7,150	11,074
Other Eurasia (OEA)	1,545	2,649
Russia (RUS)	1,977	3,219
United States of America (USA)	2,835	5,781
Western Europe (WEUR)	2,848	5,994

Source: Authors' compilation using World Health Organization (2014) data.

Africa, India, China and OAS record the highest numbers of climate-change-attributable deaths in both 2030 and 2050. While most regions experience higher mortality in 2050 than in 2030, Africa is an exception. Africa instead reflects substantial declines in undernutrition-related deaths and changes in malaria incidence across several countries by 2050 as they develop.

2.4 Energy consumption

Deviations in temperature above or below threshold levels have been shown to affect energy consumption in certain regions (Deschênes, 2022; Deschênes & Greenstone, 2011; Rode et al., 2021; Wenz et al., 2017). Empirical evidence indicates that these effects are concentrated in higher-income settings, including the top 30 per cent of countries by GDP per capita in 2019, parts of the United States, and Southern and Western Europe (Deschênes, 2022; Deschênes & Greenstone, 2011; Rode et al., 2021; Wenz et al., 2017). Changes in energy consumption are largely driven by greater usage of heating and cooling systems, with lower-income countries exhibiting smaller effects due to more limited access to such equipment (Deschênes, 2022; Rode et al., 2021). In regions where reductions in extreme cold days outweigh increases in extreme hot days, climate change may reduce overall energy consumption. This occurs because countries have a higher demand for non-electric fuels on extreme cold days than on less cold days, so when the temperature increases, less energy is required to heat homes (Deschênes, 2022; Rode et al., 2021).

2.4.1 Methodology

The Climate Impact Lab (2023) database contains data on changes in energy expenditure from electricity and other fuels in response to temperature changes driven by climate change. This is estimated using the approach in Rode et al. (2021) and Climate Impact Lab and UNDP's Human Development Report Office (n.d.), which uses international energy balance data to quantify the relationship between climate-change-induced temperature change and energy consumption. Once this relationship has been estimated from historical energy consumption data, the authors apply it to project future energy consumption under different RCP scenarios (Climate Impact Lab and UNDP's Human Development Report Office, n.d.; Rode et al., 2021). The data shows the percentage change in energy expenditure relative to GDP for each country (Climate Impact Lab , 2023).

To convert this percentage change in expenditure on energy for each country to the actual value of the expenditure on energy ($\Delta EnergyExpenditure_{c,t}$), the percentage change values are multiplied by country-level GDP ($Y_{c,2015}$).

$$\Delta EnergyExpenditure_{c,t} = [\frac{\Delta EnergyExpenditure_{c,t}}{Yc}] \cdot Y_{c,2015} \tag{5}$$

Next, this is aggregated to each region and divided by the regional GDP for 2015 to calculate the gross damages.

$$GD_{r,t,Energy} = \frac{\sum_r \Delta EnergyExpenditure_{c,t}}{Y_{r,2015}} \tag{6}$$

2.4.2 Estimates

The results indicate that climate change leads to reductions in annual total energy use in several regions, including ANZ, CAN, China, CLA, India, JSK, MEA, MEX, OEA, RUS, USA and WEUR. In most of these regions, the reduction is driven by fewer cold days. In contrast, other regions — particularly Africa, BRA, and OAS — experience increases in energy consumption in 2030 under both RCP4.5 and RCP8.5, reflecting a rise in hot days. Across all regions, there is evidence of fuel switching away from coal, oil, and natural gas towards electricity, with this effect strengthening over time.

Table 4 reports the monetary value of climate-induced changes in energy use expressed as a percentage of GDP. Under RCP4.5, the largest reductions in 2050 and 2090 occur in CAN (–0.13 per cent and –0.28 per cent), WEUR (–0.13 per cent and –0.25 per cent), and OEA (–0.10 per cent and –0.22 per cent). There are increases in energy expenditure in BRA, OAS and India in 2050 under both RCP4.5 and RCP8.5. In 2090, climate change has reduced energy expenditure as a share of GDP in AFR, ANZ, CAN, ChN, CLA, JSK, MEA, MEX, OAS, OEA, USA, and WEUR. However, in IND and BRA there is still an increase in energy expenditure in 2090.

Table 4: **Annual climate-induced change in energy expenditure as a share of GDP (%)**

	2050		2090	
Region	RCP4.5	RCP8.5	RCP4.5	RCP8.5
Africa (AFR)	-0.00	-0.01	-0.03	-0.16
Australia and New Zealand (ANZ)	-0.03	-0.04	-0.07	-0.12
Brazil (BRA)	0.01	0.02	0.04	0.10
Canada (CAN)	-0.13	-0.17	-0.28	-0.48
China (CHN)	-0.02	-0.02	-0.04	-0.05
Central and Latin America (CLA)	-0.05	-0.06	-0.09	-0.17
India (IND)	0.01	0.02	0.05	0.10
Japan and South Korea (JSK)	-0.08	-0.10	-0.15	-0.26
Middle East (MEA)	-0.04	-0.05	-0.08	-0.15
Mexico (MEX)	-0.02	-0.02	-0.02	-0.00
Other Asia (OAS)	0.00	0.00	-0.00	-0.05
Other Eurasia (OEA)	-0.11	-0.14	-0.23	-0.38
Russia (RUS)	-0.05	-0.07	-0.11	-0.20
United States of America (USA)	-0.04	-0.05	-0.08	-0.13
Western Europe (WEUR)	-0.13	-0.16	-0.25	-0.43

Source: Authors' compilation using Institute for Health Metrics and Evaluation (2024) data.

2.5 Labour productivity

Temperature increases above threshold levels have been found to reduce labour productivity (Dasgupta et al., 2021; Sahu et al., 2013; Schleypen et al., 2019). An explanation offered is that increased heat places additional strain on workers, raising heart rates and making it more difficult to maintain productivity (Sahu et al., 2013). The relationship between temperature and labour productivity is non-linear, as productivity also declines at temperatures below the threshold. The magnitude, sign, and functional form of this relationship vary across regions, sectors, and empirical approaches, with larger effects observed in hotter climates and in sectors with greater exposure to heat (Dasgupta et al., 2021; Kalkuhl & Wenz, 2020; Li et al., 2016; Sahu et al., 2013; Schleypen et al., 2019).

2.5.1 Methodology

The Human Climate Horizons database (Climate Impact Lab and UNDP's Human Development Report Office, 2022) provides estimates of climate change impacts on working hours across countries. These estimates are derived using the methodology of Rode et al. (2022), which first estimates the relationship between labour supply and maximum daily temperature for workers in high-risk sectors (agriculture, mining, construction, and manufacturing) and low-risk sectors. For high-risk sectors, the relationship follows an inverse U-shape, while for low-risk sectors the effect of extreme cold temperatures on labour supply is substantially smaller (Rode et al., 2022). Based on historical time-use and labour force survey data from seven countries, these estimated relationships are then used to project future changes in labour supply under RCP4.5 and RCP8.5 (SSP3) (Climate Impact Lab and UNDP's Human Development Report Office, n.d.; Rode et al., 2022).

Labour supply impacts of climate change from the Human Climate Horizons database are measured as the annual change in hours worked per worker at the country level, resulting from daily temperature variation ($\Delta LHoursPerWorker_{c,t}$) (Climate Impact Lab and UNDP's Human Development Report Office, 2022). These per-worker changes are multiplied by each country's labour force (LF_c) using data from the International Labour Organisation (2024) and then aggregated to the AD-MERGE 2.0 regions (r). Labour impacts are reported separately for high-risk and low-risk labour types, captured by the vector $LabourType$.

$$\Delta LHours_{r,t,LabourType} = \sum_{r} \Delta LHoursPerWorker_{c,t,LabourType}.LF_c \tag{7}$$

Monetary impacts are estimated by multiplying the regional change in labour hours ($\Delta LHours_{r,t}$) by the regional hourly wage (w_r). Hourly wages are derived from the International Labour Organisation (2024) dataset, aggregated to the AD-MERGE 2.0 regions and converted to constant 2015 US dollars. For Australia, New Zealand, and China, where hourly wage data are not reported in the International Labour Organisation alternative sources are used: the Austalian Bureau of Statistics (2024), Stats NZ (2025) and Ezrati (2023), respectively. Hourly wages are observed in 2015 and subsequently scaled in line with GDP growth, assuming a constant relationship between GDP and wage rates over time.

$$GD_{r,t,LabourType} = \Delta LProdHours_{r,t,LabourType}.w_r.(1.03)^{10} \tag{8}$$

The average change in wage expenditure resulting from climate-induced changes in working hours is calculated separately for high- and low-risk sectors.

$$GD_{r,t,Labour} = \frac{GD_{r,t,LowRiskLabour} + GD_{r,t,HighRiskLabour}}{2} \tag{9}$$

2.5.2 Estimates

Figure 2 shows that several regions—Africa, BRA, CLA, India, MEA, MEX, and OAS—experience declines in average annual labour hours per worker in both high-risk sectors (agriculture, construction, manufacturing and mining) and low-risk sectors. In these regions, increases in extreme hot days reduce labour supply and productivity on affected days. In contrast, regions such as CAN, JSK, RUS, and WEUR exhibit increases in labour hours across both sector types under RCP4.5, reflecting reductions in extreme cold days and associated productivity gains. The increase in labour hours is substantially larger in high-risk sectors, as the relationship between maximum daily temperature and labour supply shows a much stronger response to extreme cold in these sectors, while effects are comparatively modest for low-risk sectors (Rode et al., 2022). Consequently, reductions in extreme cold days generate larger gains in labour hours per worker in high-risk sectors than in low-risk sectors.

OEA and the USA exhibit both increases and decreases in labour productivity depending on whether high-risk or low-risk sectors are considered. In both regions, reductions in extreme cold days are associated with higher labour productivity in high-risk sectors under RCP4.5, reflecting the steep decline in labour hours experienced in these sectors during extreme cold conditions. As the frequency of extreme cold days falls, the resulting gains in labour hours can outweigh losses associated with higher temperatures. In contrast, in low-risk sectors, increases in extreme hot days reduce labour hours, and this effect may dominate the productivity gains from fewer extreme cold days, leading to a net decline in labour hours.

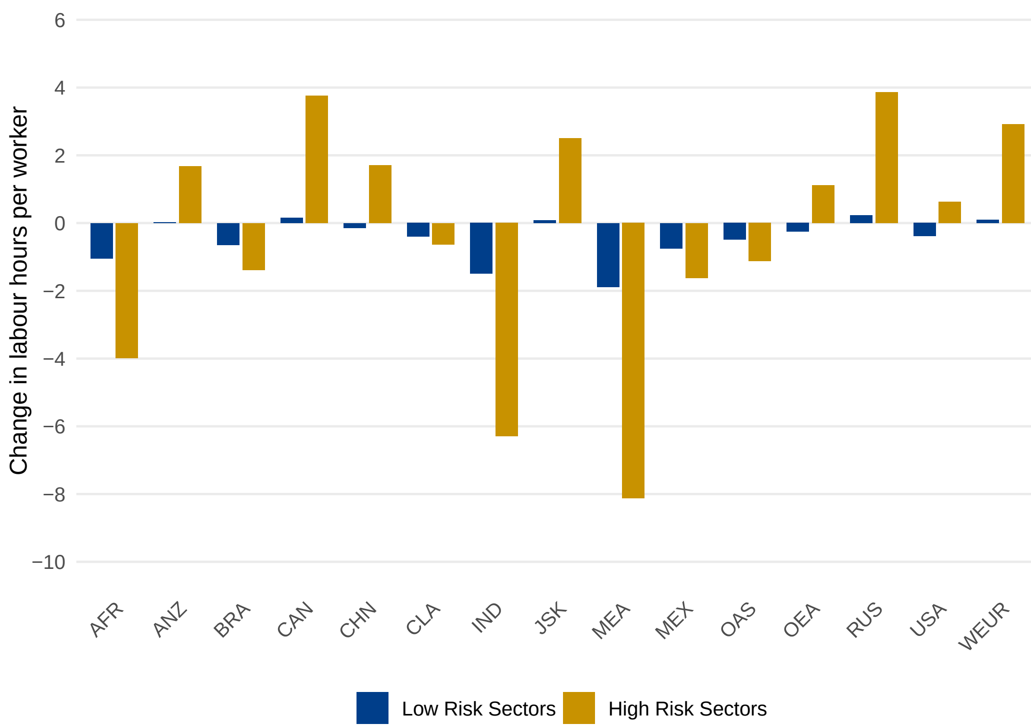

Figure 2: Average change in labour hours per worker per region from temperature changes for 2050 RCP4.5

Source: Authors' calculations based on data from Climate Impact Lab and UNDP's Human Development Report Office (2022) for countries that International Labour Organisation (2024) has labour force data.

2.6 Tourism

Temperature increases and precipitation changes can result in reductions in tourism demand in regions that already experience high temperatures or face declining snowfall (Schleypen et al., 2019; Steiger, Scott, Abegg, Pons, & Aall, 2019; Yu et al., 2009). This reflects changes in destination choice, as tourists substitute towards cooler locations or areas with more reliable snow conditions (Serquet & Rebetez, 2011; Steiger et al., 2019). Conversely, some regions may experience increases in tourism as temperatures rise (Serquet & Rebetez, 2011; Yu et al., 2009). Given the importance of tourism in many economies, climate-induced changes in tourist arrivals can have substantial implications for GDP, with adverse effects in regions where tourism demand declines.

Research on the effects of climate change on tourism remains limited. Hamilton et al. (2005) develop an econometric framework to estimate the impact of temperature changes on international tourist flows, controlling for coastline length, land area, and GDP per capita. Roson and Sartori (2016) similarly examine the effect of temperature on international tourism, incorporating country-specific fixed effects to account for unobserved factors influencing tourism demand. Rosselló-Nadal and He (2020) extend this approach by additionally accounting for visa requirements and the presence of World Heritage Sites.

2.6.1 Methodology

To quantify the impact of climate change on tourism, an econometric framework is required to estimate how alternative temperature scenarios affect tourist arrivals and, in turn, tourism income. This paper adopts the model developed by Hamilton, Maddison, and Tol (2005) which specifies the natural logarithm of international tourism arrivals (TA) as a function of average temperature (T) and its square, coastline length ($Coast$), land area ($Area$), and the natural logarithm of GDP per capita Y. The latter is used as a proxy for a country's level of economic development. The Hamilton et al. (2005) specification is applied at the AD-MERGE 2.0 regional level. Average temperature data are drawn from Our World in Data (n.d.), while data on land area, international tourist arrivals, GDP per capita, international tourism receipts, and tourism income are obtained from the World Development Indicators dataset (The World Bank, 2024). Coastline length data are sourced from the CIA (2024).

The first step is to estimate the Hamilton et al. (2005) specification for the base year 2015 in order to model the natural logarithm of tourist arrivals for each region. This specification captures the effect of a 1°C change in average temperature on tourist arrivals at the country level. The inclusion of a squared temperature term allows for non-linear temperature effects.

$$lnTA_c = \alpha + \beta_1 A_c + \beta_2 Coast_c + \beta_3 T_c + \beta_4 T_c^2 + lnY_c \tag{10}$$

The estimated coefficients from the econometric model are subsequently used to project future tourist arrivals by country and region, following an approach similar to de Bruin and Ayuba (2020). Tourist arrivals are simulated under alternative climate change scenarios using the equation below, where tco_i refers to the potential temperature increase under climate change and takes values of 0 (no climate change), 0.6, 0.8, 1, 1.4, 1.8, 2, and 3.7. Separate equations are specified for each AD-MERGE 2.0 region with more than one country, with coefficients fixed at their econometrically estimated values. Regions with only one country are included in similar regions for the sake of estimating the coefficients.

$$TA_{c,i,t} = exp(\alpha_r + \beta_{1,r} + \beta_{2,r} Coast_c + \beta_{3,r}(T_c + tco_i) + \beta_{4,r}(T_c + tco_i)_c^2 + lnY_{c,t} \tag{11}$$

Next, income per tourist arrival ($IncTA$) is estimated for the 2015 base year of AD-MERGE 2.0 as:

$$IncTA_c = \frac{TotalTourismIncome_{c,2015}}{TA_{c,2015}} \tag{12}$$

This value is then used to compute total tourism income for each country under each climate scenario:

$$TotalTourismIncome_{c,i,t} = TA_{c,i,t} \cdot IncTA_c \tag{13}$$

Climate-change-induced changes in tourism income are defined as the difference between tourism income under each scenario and the no climate change baseline:

$$\Delta TotalTourismInc_{r,i,t} = TotalTourismIncome_{c,i,t} - TotalTourismIncome_{c,0,t} \tag{14}$$

This change represents gross damages associated with tourism:

$$GD_{r,i,t} = \Delta TotalTourismInc_{r,i,t} \tag{15}$$

Finally, gross tourism damages are expressed as a percentage of regional GDP.

2.6.2 Estimates

Figure 3 reports changes in international tourist arrivals (in millions) under a 2°C warming scenario relative to a no climate change baseline for 2030 and 2050, by region. Regional estimates are constructed from countries for which data are available. Africa experiences the largest decline in international tourist arrivals under the 2°C warming scenario, while WEUR records the largest increase. This pattern is consistent with the literature documenting a reallocation of international tourism away from historically warmer destinations towards regions that have traditionally experienced cooler climates (Hamilton et al., 2005; Schleypen et al., 2019; Yu et al., 2009).

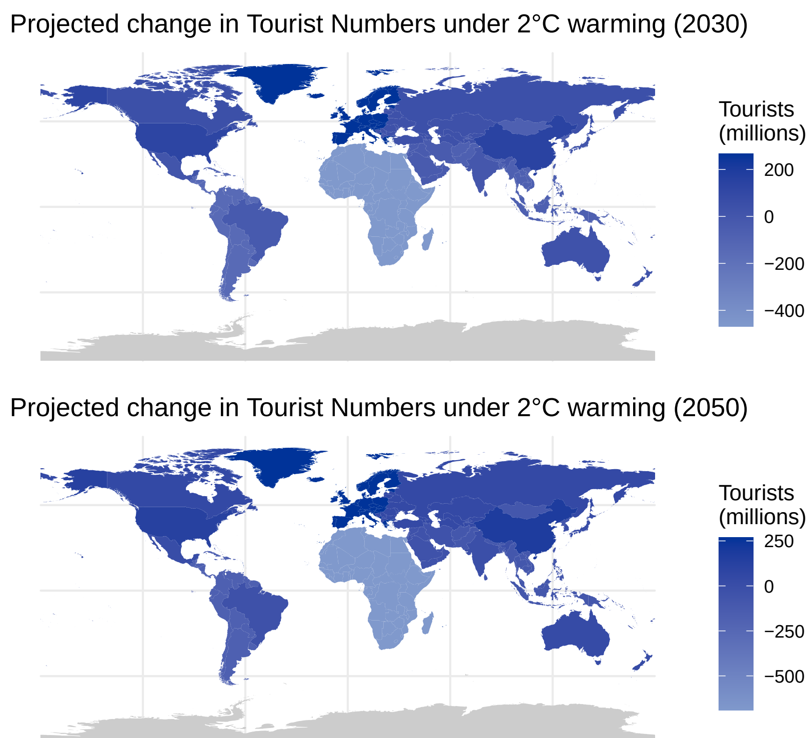

Figure 3: Change in tourist arrivals by region and time for 2 °C warming relative to no climate change

Source: Authors' calculations

Other regions experiencing declines in tourist arrivals include BRA, India, MEA, and OAS. These regions are characterised by historically warmer climates, and a 2 °C increase in temperature further intensifies heat exposure, reducing their attractiveness to tourists. As a result, tourists choose destinations with cooler average temperatures. In contrast, tourist arrivals increase in ANZ, CAN, China, JSK, MEX, OEA, RUS, and the USA. But, the use of country-level average temperatures, which are used to get these regional averages, masks within-country spatial variation in climate conditions, as highlighted by Yu et al. (2009). Future research could address these limitations by explicitly modelling seasonal and sub-national temperature effects on tourism demand.

3 Calibrating damage functions

In the AD-MERGE 2.0 model, gross damages are modelled as a function of temperature change. Adaptation can be applied to reduce these gross damages to residual damage at a cost (de Bruin, Dellink, & Tol, 2009a). AD-MERGE 2.0 considers two types of adaptation based on the timing of their costs and benefits. Stock adaptation requires a beforehand investment in adaptation capital that can reduce gross damages over multiple time periods. This reflects adaptation measures that take time to build, i.e. proactive adaptation, e.g., the building of sea walls to combat sea level rise. Flow adaptation costs and benefits fall within the same time period and reflect reactive adaptation, e.g. the application sunscreen or use of mosquito nets.

Once monetary damages are expressed as a share of GDP for each impact category, as discussed above, these estimates are aggregated by region (r), and by temperature increase (T) and time period (t) as defined in the relevant climate change scenario. These data points are used to calibrate the gross damage function based on temperature change.

$$GD_{r,t} = \alpha_{1,r} T_t^{\alpha_{2,r}} + \alpha_{3,r} T_t^{\alpha_{4,r}} \tag{16}$$

To calibrate the specific α parameters ($\alpha_{1,r}$, $\alpha_{2,r}$, $\alpha_{3,r}$, $\alpha_{4,r}$) in equation 16, we plot each region's gross damage data points on a separate graph. As an example, we show the data points for Africa in Figure 4 (navy dots). The α parameters are calibrated such that the gross damage function (equation 16) replicates the data as closely as possible. The light blue line in the figure represents this gross damage function, the previously estimated gross damage function (AD-MERGE 1.0) is shown for comparison (orange line). The clear difference between the AD-MERGE 1.0 and AD-MERGE 2.0 functions highlight the need to update damage functions as data becomes available.

The resulting regional gross damage functions may exhibit either linear or non-linear responses to temperature changes as the damages from the different impacts developed differently over temperature change and economic growth. Figure 5 illustrates the calibrated gross damage functions for the fifteen regions, with the country composition of each region reported in Table A.5 in Appendix A.

The gross damage functions are steepest for the OAS and AFR regions. This indicates that when global temperatures increase, these regions experience the largest increase in gross damages relative to GDP compared to the other regions. These regions also have lower GDP per capita values than other regions such as WEUR, the USA, ANZ and JSK. This pattern highlights the unequal distribution of climate change impacts, with lower-income regions experiencing greater damages as a share of GDP than higher-income regions, raising important considerations related to climate equity.

While region-specific gross damage functions provide important insights, aggregating them into a global gross damage function facilitates comparison with the international literature. This is particularly relevant given differences across IAMs in regional resolution and composition. The aggregated global gross damage function is therefore compared with those employed in other integrated assessment models in Figure 6.

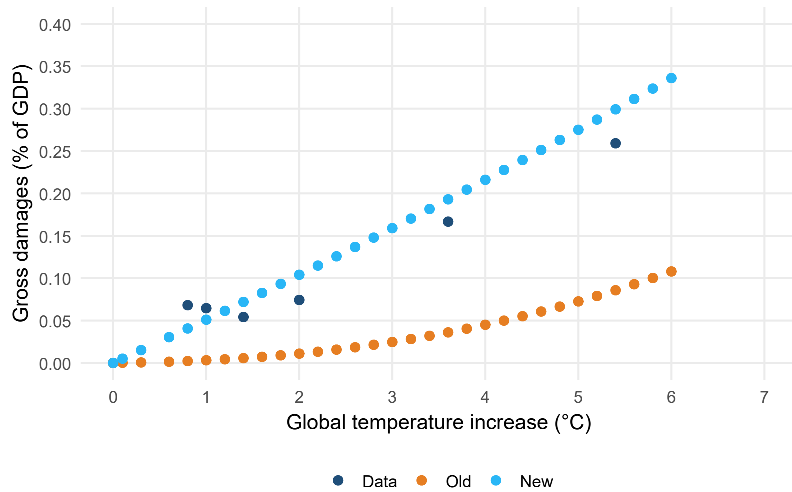

Figure 4: Calibration of the African damage function

Source: Authors' calculations

[Note to John: We're going to redo this graph to match the formatting of the other ones - just haven't had a chance yet]

The AD-MERGE 2.0 gross damage function is steeper than its predecessor in AD-MERGE 1.0, reflecting the incorporation of updated impact estimates presented in this paper, which imply larger damages per 1°C increase in global temperature. The updated function lies between the two damage functions reported by Howard and Sterner (2017), one of which includes damages from catastrophic events, while the other excludes them. Earlier damage functions developed by Tol (2009), Tol (2014) and Nordhaus (2013) are notably less steep than both the Howard and Sterner (2017) and the AD-MERGE 2.0 functions. Taken together, these comparisons indicate that successive updates to impact estimates have led to progressively steeper global damage functions. van der Wijst et al. (2023), using a quantile regression approach based on damages incorporated into a computable general equilibrium model, estimate substantially steeper temperature–damage relationships than those implied by Howard and Sterner (2017) and AD-MERGE 2.0 as illustrated by Figure 6.

4 Calibrating adaptation

Adaptation was first included in an IAM (PAGE) by Hope, Anderson, and Wenman (1993) as a simple binary choice. The explicit modelling of adaptation developed, where reactive (flow) adaptation was introduced into the DICE model (de Bruin, Dellink, & Agrawala, 2009; de Bruin, Dellink, & Tol, 2009a) and the RICE model (de Bruin, Dellink, & Agrawala, 2009; de Bruin, Dellink, & Tol, 2009b). Proactive (stock) adaptation was implemented in the FEEM-RICE model by Bosello (2010). Since then, both proactive and reactive adaptation have been implemented in AD-DICE (Agrawala et al., 2011), AD-RICE (de Bruin, 2014), AD-MERGE (Bahn et al., 2019) and AD-WITCH (Agrawala et al., 2011; Bosello et al., 2010). Models that include both proactive and reactive adaptation have also included: investment in research and development for adaptation (Bosello et al., 2010), and adaptation finance transfers (de Bruin, Dellink, & Tol, 2009b).

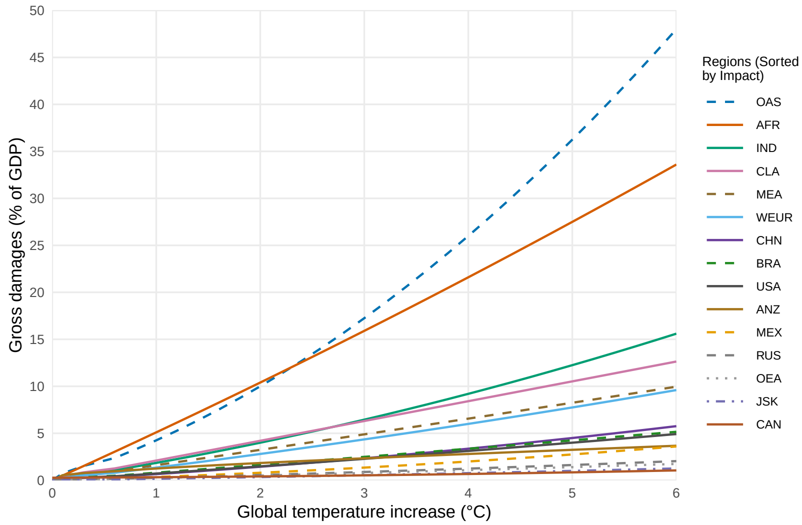

Figure 5: Regional climate change gross damage functions

Source: Authors' calculations

A second strand of the literature has focused on quantifying a region's capacity to adapt using socioeconomic indicators (Andrijevic, Byers, Mastrucci, Smits, & Fuss, 2021; Andrijevic et al., 2023). Whilst using econometrics to estimate adaptive capacity is a newer approach, adaptive capacity was implemented alongside proactive and reactive adaptation in AD-WITCH by Agrawala et al. (2011).

This paper follows the first strand of the literature and distinguishes between two types of adaptation: reactive (flow) adaptation and proactive (stock) adaptation. Flow (reactive) adaptation refers to expenditures that reduce gross climate damages in the same period in which the costs are incurred, with benefits that do not persist over time. An example is the purchase and use of sunscreen, which provides protection only in the period in which it is applied. Stock (proactive) adaptation involves investment in capital that reduces climate gross damages over future periods. Such investments may be undertaken over multiple periods in anticipation of future climate impacts and depreciate over time. An example is investment in coastal protection infrastructure, such as sea walls, to reduce gross damage from future sea level rise.

For each impact category and region, both stock and flow adaptation options are available. Calibrating adaptation effects requires information on adaptation costs for both adaptation types, as well as estimates of their effectiveness in reducing gross damages. Residual damages ($RD_{r,t}$) are defined as the damages that remain after protection measures have been applied. In this paper, adaptation costs and residual damages associated with stock and flow adaptation are calibrated using available data and evidence from the literature as outlined in the following subsections. The lack of data on regional adaptation costs and benefits for different impact types, necessitates assumptions and expert judgement in some cases (de Bruin, Dellink, & Tol, 2009a, 2009b; United Nations Environment Programme, 2023, 2025b). In what follows, we first outline our adaptation framework and then discuss each impact.

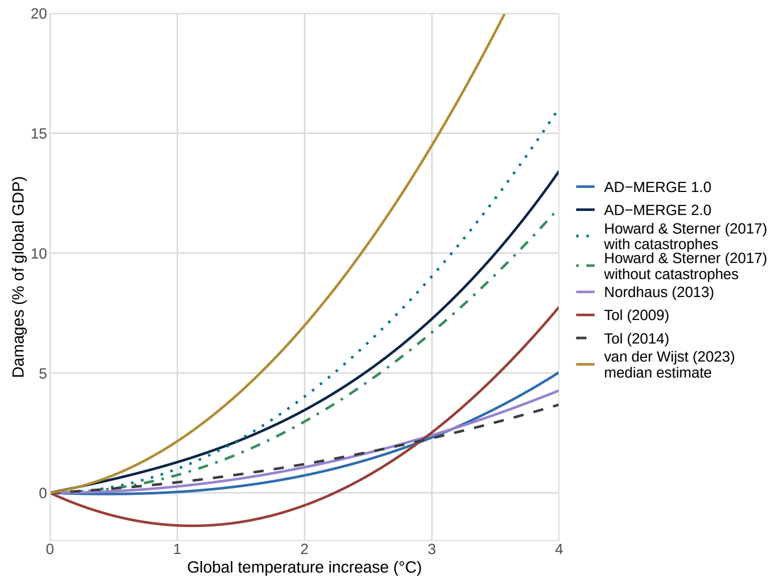

Figure 6: Comparison of global damage functions from climate change

Source: Author's calculations

4.1 Adaptation functions

Adaptation costs and benefits are described in the model through an adaptation function and a residual damage function. Adaptation $PT_{r,t}$[1] reduces gross damages ($GD_{r,t}$) into residual damages ($RD_{r,t}$):

$$RD_{r,t} = \frac{GD_{r,t}}{1 + PT_{r,t}} \tag{17}$$

This functional form ensures diminishing marginal benefits of total adaptation $PT_{r,t}$.

$PT_{r,t}$ represents the effectiveness of total adaptation, combining adaptation capital stock ($SAD_{r,t}$) and flow adaptation expenditures ($FAD_{r,t}$), both defines as a percentage of GDP. How these two adaptation types interact to determine total adaptation is described by a constant elasticity of substitution (CES) function:

$$PT_{r,t} = \beta_{1,r}(\beta_{2,r} SAD^{\rho}_{r,t} + (1 - \beta_{2,r}) FAD^{\rho}_{r,t})^{\beta_{1,r}\rho} \tag{18}$$

where adaptation stock is built up by investments ($IAD_{r,t}$) and depreciates over time by δ_k:

$$SAD_{r,t+1} = (1 - \delta_k) SAD_{r,t} + IAD_{r,t} \tag{19}$$

Each of the parameters in equation 18 describe an aspect of the trade-offs between adaptation costs, benefits and adaptation types. A higher $\beta_{1,r}$ reflects a higher effectiveness of both adaptation types. A

[1] PT reflects the damage reduction effectiveness of total adaptation (stock and flow), but is a model construct, which does not have an intuitive real world interpretation.

higher $\beta_{2,r}$ reflects a higher effectiveness of stock adaptation. $\beta_{3,r}$ parameters reflects the changes in marginal effectiveness of adaptation as it increases. And the elasticity of substitution between stock and flow adaptation is given by σ, where:

$$\rho = \frac{\sigma - 1}{\sigma} \tag{20}$$

To calibrate this function we need data on the optimal adaptation levels (defined as fraction of gross damage reduced) and the associated cost for each adaptation type for each impact. We aggregate these adaptation costs and adaptation benefits across impact categories to obtain the total adaptation stock and flow adaptation expenditure in each region for different temperature levels.

Similarly to gross damages, we calibrate the adaptation parameters to fit the data. Calibrating the adaptation function is more complex as we have multiple variables (stock and flow adaptation), which are substitutes. Trade offs between stock and flow adaptation is calibrated using the estimated adaptation costs and effectiveness of one form of adaptation when the other form is not applied.

4.2 Coastal flooding adaptation

The CIAM model (Diaz, 2016) includes two types of adaptation, the first is proactive measures such as building sea walls, whilst the second is to retreat from the flood prone areas. The model splits coastlines into multiple segments. Various adaptation scenarios can be run, including optimal adaptation, (where adaptation is optimised within each segment) and different flood protection levels. We aggregate adaptation and protection cost data by region and scenarios for both adaptation types. The detail of the CIAM allows us to collect all the necesary data without the need for additional assumptions.

4.3 River flooding adaptation

The Aqueduct Floods tool from the World Resources Institute (Ward et al., 2020; World Resources Institute, 2020) is an interactive tool that allows users to see the costs and benefits of different levels of river flooding protection for all nations. This tool is calibrated based on data from the Global Flood Risk with IMAGE Scenarios (GLOFRIS) (Winsemius et al., 2013; Winsemius et al., 2016). We follow a similar approach to Subsection 2.2, except that we extract cost-benefit data for each country and each scenario at relevant protection levels from the Aqueduct Floods tool. We then aggregate the data by region to get the final costs and benefits of flood protection. There are two types of flood adaptation: stock adaptation (such as river dykes) and flow adaptation (such as sandbag deployment). We split the regional flood protection costs and benefits into stock and flow adaptation.

4.4 Health adaptation

Very little data is available concerning adaptation costs and benefits of health impacts. Cost-effective solutions exist for diarrhoea, malaria, dengue and heat stress, though the scale of adoption varies by solution and region. Walker et al. (2011) shows that numerous low-cost solutions exist to prevent mortality from diarrhoeal diseases, including vitamin supplements, improved sanitation, water and handwashing, as well as the rotavirus vaccine. The authors model two scenarios where they increase adoption of these solutions and estimate the costs and benefits (child mortality reductions) relative to the baseline scenario (Walker et al., 2011). Malaria can be prevented by measures such as taking antimalarial medication, using insecticide-treated mosquito nets, and spraying insecticide repellents (World Health Organisation, 2021). Ralaidovy, Lauer, Pretorius, Briet, and Patouillard (2021) show the cost of preventing malaria through the use of insecticide-treated nets or the vaccine for malaria. Both interventions are low-cost compared to treating someone with a severe case of malaria, but they are more expensive than treating someone with an uncomplicated case of malaria (Ralaidovy et al., 2021). However, in all cases prevention and treatment cost are far smaller than the cost of a death.

Fitzpatrick et al. (2017) compare the cost of the dengue vaccine and vector control costs with the costs of treating someone with dengue (clinic and hospital costs) in Brazil, Mexico, Colombia, Malaysia, the Philippines and Thailand. The authors show that whilst the strategy of using vaccines and vector control is most cost-effective across all countries, the costs vary by country (Fitzpatrick et al., 2017). Effective adaptations to heat-stress mortality include early warning systems, air conditioners and district cooling (Hyyrynen et al., 2025; Sera et al., 2020; Toloo, FitzGerald, Aitken, Verrall, & Tong, 2013). However, access to air conditioners varies across countries (Andrijevic et al., 2021).

Whilst lower-cost reactive adaptation solutions are available to prevent diarrhoea, malaria, dengue and heat, there is still a need to invest in health infrastructure. This is because, as mosquitoes expand their territory, droughts affect food production and heatwaves occur, leading to an increase in hospitalisations despite preventative measures in some regions. Investment in health infrastructure is needed to support patients and strengthen the healthcare system's resilience to climate change (Ansah, Amoadu, Obeng, & Sarfo, 2024). Examples of adaptation include measures that improve water access, such as a backup supply of clean water, ventilation to prevent mosquitoes from entering the hospital, and early warning systems for health outbreaks (World Health Organisation, 2020). These investments are expensive but yield co-benefits. However, the strategies that high-income countries have followed to improve health infrastructure have differed from those of low and middle-income countries (Ansah et al., 2024). This shows the need to investigate adaptation strategies and costs at a regional or country level.

Adaptation can be effective at reducing the increase in malnutrition from climate change (Nelson et al., 2009; Sulser et al., 2021). This adaptation can take the form of reactive adaptation (helping farmers be more efficient) to proactive adaptation (water infrastructure and transport infrastructure development) (Nelson et al., 2009; Sulser et al., 2021). The adaptation costs vary depending on the type of measure (Sulser et al., 2021).

These studies have shown the variety of adaptation options, their costs, and how these costs may vary across countries. We use available research and expert judgment to determine the aggregate adaptation costs and adaptation benefits across the different regions based on their specific health impact, geography and development level.

4.5 Labour productivity adaptation

Different measures can be taken to help the labour force adapt to increases in temperature. These include providing air conditioning, shade, early warning systems, educational campaigns on coping, and working-hour changes (Day, Fankhauser, Kingsmill, Costa, & Mavrogianni, 2019). Some of these measures have higher benefit-to-cost ratios than others (Day et al., 2019). In subsection 2.5, we explained that we consider high-risk (agriculture, mining, construction and manufacturing) and low-risk sectors (the remaining sectors). Because many high-risk sectors involve working outdoors or in difficult-to-cool areas, this limits the types of adaptation measures available, where adaptation will have limits and there will be days too hot to work. As such, we assume that these sectors have lower adaptation potential than the low-risk sectors, particularly in Africa, India and the MEA. An example of this is that an office worker can use an air conditioner to cool down, whilst a farmworker with limited shade options may find it harder to cool down (Day et al., 2019). United Nations Environment Programme (2023) note that they do not include the adaptation costs for labour productivity. This may be due to a lack of empirical data detailing the costs of labour productivity adaptation measures across countries. We do include adaptation costs for this impact category. We do this by assuming that the adaptation costs vary across regions due to differences in affordability, technology accessibility and the prices of goods and labour. We use the available information on adaptation options and expert judgement to determine the final adaptation costs and adaptation in each region.

4.6 Tourism adaptation

Adaptation in the tourism sector varies from creating artificial snow to attracting more domestic tourists in different months of the year to investing in technologies to allow access to water in a drought or improve cooling in hotels (Dube & Nhamo, 2018; Dube, Nhamo, & Chikodzi, 2022; Serquet & Rebetez, 2011; Steiger et al., 2019). Different adaptation measures will be needed in different countries, and their costs are likely to vary accordingly. As a result, the empirical calibration of adaptation costs and adaptation potential in the tourism sector was based on expert judgement and the literature on adaptation options in the sector. Unlike this working paper, United Nations Environment Programme (2023) and (United Nations Environment Programme, 2025a) exclude adaptation costs from tourism in their modelled adaptation costs.

4.7 Validation

Estimating climate damages and adaptation costs at this scale is limited by the access to reliable data. Gaining an understanding of climate impacts at a global scale and of regional differences is of paramount importance. Hence, in this paper we tackle these data limitations as best as possible to gain insights into global climate impacts. Concerns regarding data and assumptions will always remain necesitating detailed accounts and comparisons with other estimates. To validate our results, our modelled adaptation costs were compared with their equivalent in the United Nations Environment Programme (2025b). The Adaptation Gap Report (United Nations Environment Programme, 2025b) estimates the modelled adaptation costs for developing countries. The sectors that both this paper and United Nations Environment Programme (2025b) estimate are: coastal, river flooding and health. This paper also includes adaptation costs for labour productivity and tourism, which are not included in (United Nations Environment Programme, 2025b). Instead, they include adaptation in: agriculture, infrastructure, fisheries, the marine environment, biodiversity and ecosystems, industry, and disaster risk reduction (United Nations Environment Programme, 2025b). Because this paper includes all nations, whereas United Nations Environment Programme (2025b) includes only developing nations, the rankings of regions will be compared rather than the exact values of the modelled costs. The regional ranking of modelled costs is OEA<MEA<CLA<OAS<Africa in this paper and OEA<MEA<Africa<CLA<OAS in United Nations Environment Programme (2025b). As such, the ranking is the same for OEA<MEA<Africa, but the ranked positions of CLA and OAS vary. United Nations Environment Programme (2025a, 2025b) also contain data on adaptation finance needs, when regions are ranked by this they are: OEA<MEA<CLA<Africa<OAS. This ranking is even more similar to the one in this paper, except for the position of OAS. However, according to United Nations Environment Programme (2025b), the adaptation finance needs for OAS are largely dependent on infrastructure, water,

biodiversity and agriculture, which are not considered in our paper. The sectors with the greatest adaptation finance needs in Africa are covered in this paper. This explains why our paper has higher adaptation costs for Africa than OAS. This comparison has confirmed that the regional ranking of our modelled costs aligns with the literature for most regions, and we understand why any differences occur.

5 Conclusion

This paper presents updated climate change gross damage functions constructed using the latest publicly accessible data. The underlying data sources and methodological procedures are documented in detail, and the resulting gross damage functions are reported to facilitate their use in future research.

The analysis quantifies climate change impacts across six categories: sea level rise, river flooding, morbidity and mortality, energy consumption, labour productivity and tourism. These impacts vary by region, temperature increase, and emissions scenario, and are used to calibrate both linear and non-linear gross damage functions. A comparison across AD-MERGE 2.0 regions indicates that gross damages as a share of GDP are higher for a given temperature increase in Africa and the Other Asian States than in other regions. At the global level, the estimated damage function aligns closely with the specifications reported by Howard and Sterner (2017), both with and without catastrophic risk components.

Adaptation is modelled as comprising proactive (stock) and reactive (flow) components. For each region and impact category, adaptation costs and the corresponding reductions in gross damages are estimated, thereby updating the adaptation parameters used in the literature.

References

Abatzoglou, J. T., & Williams, A. P. (2016). Impact of anthropogenic climate change on wildfire across western US forests. *Proceedings of the National Academy of Science (PNAS)*, *113*, 11770–11775.

Agrawala, S., Bosello, F., Carraro, C., de Bruin, K., De Cian, E., Dellink, R., & Lanzi, E. (2011). Plan or react? analysis of adaptation costs and benefits using integrated assessment models. *Climate Change Economics*, *2*(03), 175–208. doi: https://doi.org/10.1142/S2010007811000267

Amirmoeini, K., Bahn, O., de Bruin, K., Everett, K., Kouchaki-Penchah, H., & Pineau, P.-O. (2026). Ad-merge 2.0: An integrated assessment of the nexus among energy transitions, climate impacts, and adaptation responses. *EGUsphere*, *2026*, 1–40.

Andrijevic, M., Byers, E., Mastrucci, A., Smits, J., & Fuss, S. (2021). Future cooling gap in shared socioeconomic pathways. *Environmental Research Letters*, *16*(9), 094053. doi: https://doi.org/10.1088/1748-9326/ac2195

Andrijevic, M., Schleussner, C.-F., Crespo Cuaresma, J., Lissner, T., Muttarak, R., Riahi, K., … Byers, E. (2023). Towards scenario representation of adaptive capacity for global climate change assessments. *Nature Climate Change*, *13*(8), 778–787. doi: https://www.nature.com/articles/s41558-023-01725-1

Ansah, E. W., Amoadu, M., Obeng, P., & Sarfo, J. O. (2024). Health systems response to climate change adaptation: a scoping review of global evidence. *BMC public health*, *24*(1), 2015. doi: https://doi.org/10.1186/s12889-024-19459-w

Arnell, N. W., & Gosling, S. N. (2016). The impacts of climate change on river flood risk at the global scale. *Climatic Change*, *134*, 387–401. doi: https://www.doi.org/10.1007/s10584-014-1084-5

Auffhammer, M. (2018). Quantifying economic damages from climate change. *Journal of Economic Perspectives*, *32*(4), 33–52. doi: https://doi.org/10.1257/jep.32.4.33

Austalian Bureau of Statistics. (2024). *Employee earnings and hours, australia.* (`https://www.abs.gov.au/statistics/labour/earnings-and-working-conditions/employee-earnin` accessed March 2025)

Baccini, M., Biggeri, A., Accetta, G., Kosatsky, T., Katsouyanni, K., Analitas, A., … Michelozzi, P. (2008). Heat Effects on Mortality in 15 European Cities. *Epidemiology*, *19*, 711-719. doi: https://doi.org/10.1097/EDE.0b013e318176bfcd

Bahn, O., Bruin, K. d., & Fertel, C. (2019). Will adaptation delay the transition to clean energy systems? an analysis with ad-merge. *The Energy Journal*, *40*(4), 207–234. doi: https://doi.org/10.5547/01956574.40.4.obah

Bandyopadhyay, S., Kanji, S., & Wang, L. (2012). The impact of rainfall and temperature variation on diarrheal prevalence in Sub-Saharan Africa. *Applied Geography*, *33*, 63–72. doi: https://www.doi.og/10.1016/j.apgeog.2011.07.017

Bosello, F. (2010). *Adaptation, mitigation and'green'r&d to combat global climate change. insights from an empirical integrated assessment exercise* (Tech. Rep. No. 22.2010). FEEM. `https://ssrn.com/abstract=1573633`.

Bosello, F., Carraro, C., & De Cian, E. (2010). Climate policy and the optimal balance between mitigation, adaptation and unavoided damage. *Climate Change Economics*, *1*(02), 71–92. doi: https://doi.org/10.1142/S201000781000008X

Bosetti, V., Carraro, C., Galeotti, M., Massetti, E., & Tavoni, M. (2006). A world induced technical change hybrid model. *The Energy Journal*, *27*(2_suppl), 13–37. doi: https://doi.org/10.5547/ISSN0195-6574-EJ-VolSI2006-NoSI2-2

Breitner, S., Wolf, K., Devlin, R. B., Diaz-Sanchez, D., Peters, A., & Schneider, A. (2014). Short-term effects of air temperature on mortality and effect modification by air pollution in three cities of Bavaria, Germany: A time-series analysis. *Science of the Total Environment*, *485-486*, 49–61. doi: https://doi.org/10.1016/j.scitotenv.2014.03.048

Caminade, C., Kovats, S., Rocklov, J., Tompkins, A. M., Morse, A. P., Colón-Gonzaléz, F. J., … Lloyd, S. J. (2014). Impact of climate change on global malaria distribution. *Proceedings of the National Academy of Sciences (PNAS)*, *111*, 3286–3291. doi: https://doi.org/10.1073/pnas.1302089111

Carlton, E., Woster, A. P., DeWitt, P., Goldstein, R. S., & Levy, K. (2016). A systematic review and meta-analysis of ambient temperature and diarrhoeal diseases. *International Journal of Epidemiology*, 117-130. doi: https://www.doi.org/10.1093/ije/dyv296

Chapman, S., Birch, C. E., Marsham, J. H., Part, C., Hajat, S., Chersich, M. F., … Kovats, S. (2022). Past and projected climate change impacts on heat-related child mortality in africa. *Environmental Research Letters*, *17*(7), 074028. doi: https://doi.org/10.1088/1748-9326/ac7ac5

Chou, W., Wu, J., Wang, Y., Huang, H., Sung, F., & Chuang, C. (2010). Modeling the impact of climate variability on diarrhea-associated diseases in Taiwan (1996-2007). *Science of the Total Environment*, *409*, 43–51. doi: https://www.doi.org/10.1016/j.scitotenv.2010.09.001

CIA. (2024). *Field Listing - Coastline.* (`https://www.cia.gov/the-world-factbook/field/coastline/`, accessed 2024-06-04)

Climate Impact Lab. (2023). *Impact map.* (`https://impactlab.org/map/usmeas=absoluteusyear=1986-2005&gyear=2020-2039&tab=globalgpro` accessed 22-01-2026)

Climate Impact Lab and UNDP's Human Development Report Office. (n.d.). *Methodology.* (`https://horizons.hdr.undp.org/HCH`$_{M}ethodology_{U}NDP_{C}IL.pdf, accessedMay$2024)

Climate Impact Lab and UNDP's Human Development Report Office. (2022). *Human climate horizons: Compare impacts.* (`https://www.horizons.hdr.undp.org//risk`)

Cline, W. R. (1992). *The economics of global warming*. Washington, D.C.: Institute for International Economics.

Dasgupta, S., van Maanen, N., Gosling, S. N., Piontek, F., Otto, C., & Schleussner, C.-F. (2021). Effects of climate change on combined labour productivity and supply: an empirical, multi-model study. *Lancet Planet Health*, *5*, e455-e465.

Day, E., Fankhauser, S., Kingsmill, N., Costa, H., & Mavrogianni, A. (2019). Upholding labour productivity under climate change: an assessment of adaptation options. *Climate policy*, *19*(3), 367–385. doi: https://doi.org/10.1080/14693062.2018.1517640

de Bruin, K. (2014). *Calibration of the ad-rice 2012 model* (Tech. Rep. No. 2014:3). CERE. `https://dx.doi.org/10.2139/ssrn.2600006`.

de Bruin, K., & Ayuba, V. (2020). *What does paris mean for africa? an integrated assessment analysis of the effects of the paris agreement on african economies* (Tech. Rep. No. 690). Dublin: Economic and Social Research Institute. `https://www.esri.ie/publications/what-does-paris-mean-for-africa-an-integrated-assessment`

de Bruin, K., Dellink, R., & Agrawala, S. (2009). *Economic aspects of adaptation to climate change: integrated assessment modelling of adaptation costs and benefits* (Tech. Rep. No. 2009:1). OECD Publishing.

de Bruin, K., Dellink, R., & Tol, R. (2009a). Ad-dice: an implementation of adaptation in the dice model. *Climatic Change*, *95*(1), 63–81. doi: https://doi.org/10.1007/s10584-008-9535-5

de Bruin, K., Dellink, R., & Tol, R. (2009b). *International cooperation on climate change adaptation from an economic perspective* (Tech. Rep. No. 323). ESRI. `https://hdl.handle.net/10419/50142`.

Depsky, N., Bolliger, I., Allen, D., Ho Choi, J., Delgado, M., Greenstone, M., … Hsiang, S. (2023). DSCIM-Coastal v1.1: an open-source modeling platform for global impacts of sea level rise. *Geoscientific Model Development*, *16*, 4331–4366. doi: https://www.doi.org/10.5194/gmd-16-4331-2023

Deschênes, O. (2022). The impact of climate change on mortality in the United States: Benefits and costs of adaptation. *Canadian Journal of Economics*, *55*, 1227–1249. doi: https:doi.org/10.1111/caje.12609

Deschênes, O., & Greenstone, M. (2011). Climate Change, Mortality, and Adaptation: Evidence from Annual Fluctuations in Weather in the US. *American Economic Journal: Applied Economics*, 152–185. doi: http://dx.doi.org/10.1257/app.3.4.152

Diaz, D., & Moore, F. (2017). Quantifying the economic risks of climate change. *Nature Climate Change*, *7*(11), 774–782. doi: https://doi.org/10.1038/nclimate3411

Diaz, D. B. (2016). Estimating global damages from sea level rise with the Coastal Impact and Adaptation Model (CIAM). *Climatic Change*, *137*, 143–156. doi: https:/doi.org/10.1007/s10584-016-1675-4

Dickerson, S., Cannon, M., & O'Neill, B. (2021). Climate change risks to human development in sub-Saharan Africa: a review of the literature. *Climate and Development*. doi: https://doi.org/10.1080/17565529.2021.1951644

Dottori, F., Szewczyk, W., Cisar, J.-C., Zhao, F., Alfieri, L., Hirabayashi, Y., … Feyen, L. (2018). Increased human and economic losses from river flooding with anthropogenic warming. *Nature Climatic Change*, *8*, 781–786. doi: https://doi.org/10.1038/s41558-018-0257-z

Dube, K., & Nhamo, G. (2018). Climate variability, change and potential impacts on tourism: Evidence from the zambian side of the victoria falls. *Environmental Science & Policy*, *84*, 113–123. doi: https://doi.org/10.1016/j.envsci.2018.03.009

Dube, K., Nhamo, G., & Chikodzi, D. (2022). Climate change-induced droughts and tourism: Impacts and responses of western cape province, south africa. *Journal of Outdoor Recreation and Tourism*, *39*, 100319. doi: https://doi.org/10.1016/j.jort.2020.100319

Ezrati, M. (2023). *The East-West Wage Gap Not Nearly as Compelling As it Once Was.* (`https://www.forbes.com/sites/miltonezrati/2023/01/30/the-east-west-wage-gap-not-nearly-a`

Fitzpatrick, C., Haines, A., Bangert, M., Farlow, A., Hemingway, J., & Velayudhan, R. (2017). An economic evaluation of vector control in the age of a dengue vaccine. *PLoS neglected tropical diseases*, *11*(8), e0005785. doi: https://doi.org/10.1371/journal.pntd.0005785

Grace, K., Davenport, F., Funk, C., & Lerner, A. M. (2012). Child malnutrition and climate in sub-saharan africa: An analysis of recent trends in kenya. *Applied Geography*, *35*(1-2), 405–413. doi: https://doi.org/10.1016/j.apgeog.2012.06.017

Hamilton, J. M., Maddison, D. J., & Tol, R. S. (2005). Climate change and international tourism: a simulation study. *Global environmental change*, *15*(3), 253–266. doi: https://doi.org/10.1016/j.gloenvcha.2004.12.009

Hamilton, J. M., Maddison, D. J., & Tol, R. S. (2005). Effects of climate change on international tourism. *Climate research*, *29*, 245–254. doi: https://doi.org/10.3354/cr029245

Hinkel, J. (2005). DIVA: an iterative method for building modular integrated models. *Advances in Geosciences*, *4*, 45–50. doi: https://doi.org/10.5194/adgeo-4-45-2005

Hinkel, J., & Klein, R. J. (2009). Integrating knowledge to assess coastal vulnerability to sea-level rise: The development of the DIVA tool. *Global Environmental Change*, *19*, 384-395. doi: https://www.doi.org/10.1016/j.gloenvcha.2009.03.002

Hinkel, J., van Vuuren, D. P., Nicholls, R. J., & Klein, R. J. (2013). The effects of adaptation and mitigation on coastal flood impacts during the 21st century. An application of the DIVA and IMAGE models. *Climatic Change*, *117*, 783–794. doi: https://www.doi.org/10.1016/j.gloenvcha.2009.03.002

Hope, C., Anderson, J., & Wenman, P. (1993). Policy analysis of the greenhouse effect: an application of the page model. *Energy Policy*, *21*(3), 327–338. doi: https://doi.org/10.1016/0301-4215(93)90253-C

Howard, P., & Sterner, T. (2017). Few and not so far between: a meta-analysis of climate damage estimates. *Environmental and Resource Economics*, *68*(1), 197–225. doi: https://doi.org/10.1007/s10640-017-0166-z

Hyyrynen, M., Ollikainen, M., Käyhkö, J., Suomi, J., Lintunen, J., Käyhkö, J., … Juhola, S. (2025). Cooling is a cost-efficient way to adapt to heatwaves even in high-latitude cities. *Climatic Change*, *178*(5), 96. doi: https://doi.org/10.1007/s10584-025-03913-8

Institute for Health Metrics and Evaluation. (2024). *Global burden of disease results.* Seattle. (`https://vizhub.healthdata.org/gbd-results/`, accessed 2024-06-04)

International Labour Organisation. (2024). *ILOSTAT data explorer.* (`https://rshiny.ilo.org/dataexplorer51/?lang=enid=EAR`$_{4}HRL_{S}EX_{C}UR_{N}B_{A}, accessed 2024-$ $12-03$)

IPCC. (2012). Managing the Risks of Extreme Events and Disasters to Advance Climate Change Adaptation. In (pp. 1–19). Cambridge: Cambridge University Press. (`https://www.ipcc.ch/report/managing-the-risks-of-extreme-events-and-disasters-to-advance-`

Kalkuhl, M., & Wenz, L. (2020). The impact of climate conditions on economic, production. Evidence from a global panel of regions. *Journal of Environmental Economics and Management*, *103*(102360). doi: https://doi.org/10.1016/j.jeem.2020.102360

Li, X., Hang Chow, K., Zhu, Y., & Lin, Y. (2016). Evaluating the impacts of high-temperature outdoor working environments on construction labour productivity in China: A case study of rebar workers. *Building and Environment*, 42–52. doi: https://doi.org/10.1016/j.buildenv.2015.09.005

Lincke, D., Hinkel, J., van Ginkel, K., Jeuken, A., Botzen, W., Tesselaar, M., ... Ignjacevic, P. (2018). *D2.3 Impacts on infrastructure, built environment, and transport: Deliverable of the H2020 COACCH project* (Tech. Rep.). Brussels: European Union.

Link, P. M., & Tol, R. S. (2006). *The economic impact of a shutdown of the thermohaline circulation: an application of fund* (Tech. Rep. No. 103). Hamburg: FNU.

Liu-Helmersson, J., Stenlund, H., Wilder-Smith, A., & Rocklov, J. (2014). Vectorial Capacity of Aedes aegypti: Effects of Temperature and Implications for Global Dengue Epidemic Potential. *PLoS ONE*, *9*(e89783). doi: https://www.doi.org/10.1371/journal.pone.0089783

Lloyd, S. J., Kovats, R. S., & Armstrong, B. G. (2007). Global diarrhoea morbidity, weather and climate. *Climate Research*, *34*, 119–127. doi: https://www.doi.org/10.3354/cr034119

Lloyd, S. J., Kovats, R. S., & Chalabi, Z. (2011). Climate Change, Crop Yields, and Undernutrition: Development of a Model to Quantify the Impact of Climate Scenarios on Child Undernutrition. *Environmental Health Perspectives*, *119*, 1817–1823. doi: https://doi.org/10.1289/ehp.1003311

Manne, A., Mendelsohn, R., & Richels, R. (1995). Merge: A model for evaluating regional and global effects of ghg reduction policies. *Energy policy*, *23*(1), 17–34. doi: https://doi.org/10.1016/0301-4215(95)90763-W

Mordecai, E. A., Ryan, S. J., Caldwell, J. M., Shah, M. M., & LaBeaud, A. (2020). Climate change could shift disease burden from malaria to arboviruses in Africa. *The Lancet Planetary Health*, *4*, e416–e423. doi: https://doi.org/10.1016/S2542-5196(20)30178-9

Narita, D., Tol, R. S., & Anthoff, D. (2009). Damage costs of climate change through intensification of tropical cyclone activities: an application of fund. *Climate Research*, *39*(2), 87–97. doi: https://doi.org/10.3354/cr00799

Narita, D., Tol, R. S., & Anthoff, D. (2010). Economic costs of extratropical storms under climate change: an application of fund. *Journal of Environmental Planning and Management*, *53*(3), 371–384. doi: https://doi.org/10.1080/09640561003613138

Nelson, G. C., Rosengrant, M. W., Koo, J., Robertson, R., Sulser, T., Zhu, T., ... Lee, D. (2009). *Climate Change: Impact on Agriculture and Costs of Adaptation* (Tech. Rep.). International Food Policy Research Institute. `https://play.google.com/store/books/details?id=1Vpe0JvYTJYCrdid=book-1Vpe0JvYTJYCrdot=1so` $books_booksearch_atbpli = 1$.

Nordhaus, W. (1992). *The "Dice" Model: Background and Structure of a Dynamic Integrated Climate-Economy Model of the Economics of Global Warming* (Tech. Rep. No. 1009). Conneticut: Yale University. `https://elischolar.library.yale.edu/cowles-discussion-paper-series/1252`.

Nordhaus, W. (2013). *The climate casino: Risk, uncertainty, and economics for a warming world.* Yale University Press.

Nordhaus, W., & Yang, Z. (1996). A regional dynamic general-equilibrium model of alternative climate-change strategies. *The American Economic Review*, 741–765. doi: https://www.jstor.org/stable/2118303

OECD. (2012). *Mortality Risk Valuation in Environment, Health and Transport Policies* (Tech. Rep.). Paris: OECD Publishing. https://www.oecd.org/content/dam/oecd/en/publications/reports/2012/02/mortality-risk-valu *en.pdf*.

Our World in Data. (n.d.). *Average monthly surface temperature, jan 15, 2009 to oct 15, 2009.* (https://ourworldindata.org/grapher/average-monthly-surface-temperature?tab=tabletime=200

Ralaidovy, A. H., Lauer, J. A., Pretorius, C., Briet, O. J., & Patouillard, E. (2021). Priority setting in hiv, tuberculosis, and malaria–new cost-effectiveness results from who-choice. *International Journal of Health Policy and Management*, *10*(11), 678. doi: https://doi.org/10.34172/ijhpm.2020.251

Rode, A., Baker, R. E., Carleton, T., D'Agostino, A., Delgado, M., Foreman, T., ... J., Y. (2022). *Labor Disutility in a Warmer World: The Impact of Climate Change on the Global Workforce.* doi: https://dx.doi.org/10.2139/ssrn.4221478

Rode, A., Carleton, T., Delgado, M., Greenstone, M., Houser, T., Hsiang, S., ... Yuan, J. (2021). Estimating a social cost of carbon for global energy consumption. *Nature*, *598*, 308–314. doi: https://doi.org/10.1038/s41586-021-03883-8

Rogers, D. J., & Randolph, S. (2000). The global spread of malaria in a future, warmer world. *Science*, *289*, 1763–1766. doi: https://www.doi.org10.1126/science.289.5485.1763

Roson, R., & Sartori, M. (2016). Estimation of climate change damage functions for 140 regions in the GTAP9 database. *World Bank Policy Research Working Paper*. Retrieved from https://hdl.handle.net/10278/3674450

Rosselló-Nadal, J., & He, J. (2020). Tourist arrivals versus tourist expenditures in modelling tourism demand. *Tourism Economics*, *26*, 1311–1326. doi: https://doi.org/10.1177/1354816619867810

Sahu, S., Sett, M., & Kjellstrom, T. (2013). Heat exposure, cardiovascular stress and work productivity in rice harvesters in india: Implications for a climate change future. *Industrial Health*, *51*, 424–431. doi: https://doi.org/10.2486/indhealth.2013-0006

Schleypen, J., Dasgupta, S., Borsky, S., Jury, M., Scasný, M., & Bezhanishvili, L. (2019). *D2.4 Impacts on Industry, Energy, Services, and Trade: Deliverable of the H2020 COACCH project* (Tech. Rep.). Brussels: European Union.

Seneviratne, S., Zhang, X., Adnan, M., Badi, W., Dereczynski, C., Di Luca, A., ... Zhou, B. (2021). Climate Change 2021: The Physical Science Basis. Contribution of Working Group I to the Sixth Assessment Report of the Intergovernmental Panel on Climate Change. In (p. 1513–1766). Cambridge, United Kingdom and New York, NY, USA: Cambridge University Press. doi: https://doi.org/10.1017/9781009157896.013

Sera, F., Hashizume, M., Honda, Y., Lavigne, E., Schwartz, J., Zanobetti, A., ... others (2020). Air conditioning and heat-related mortality: a multi-country longitudinal study. *Epidemiology*, *31*(6), 779–787. doi: https://doi.org/10.1097/EDE.0000000000001241

Serquet, G., & Rebetez, M. (2011). Relationship between tourism demand in the Swiss Alps and hot summer air temperatures associated with climate change. *Climatic Change*, *108*, 291–300. doi: https://www.doi.org/10.1007/s10584-010-0012-6

Siraj, A. S., Oidtman, R., Huber, J., Kraemer, M. U., Brady, O., Johansson, M., & Perkins, T. (2017). Temperature modulates dengue virus epidemic growth rates through its effects on reproduction numbers and generation intervals. *PLoS neglected tropical diseases*, *11*(e0005797). doi: https://doi.org/10.1371/journal.pntd.0005797

Skoufias, E., & Vinha, K. (2013). The impacts of climate variability on household welfare in rural mexico. *Population and Environment*, *34*(3), 370–399. doi:

https://doi.org/10.1007/s11111-012-0167-3
Song, J., Pan, R., Yi, W., Wei, Q., Song, S., Tang, C., ... Su, H. (2021). Ambient high temperature exposure and global disease burden during 1990-2019: An analysis of the Global Burden of Disease Study 2019. *Science of the Total Environment*, *787*. doi: https://doi.org/10.1016/j.scitotenv.2021.147540
Stats NZ. (2025). *Labour market statistics: March 2025 quarter.* (`https://www.stats.govt.nz/information-releases/labour-market-statistics-march-2025-quart`
Steiger, R., Scott, D., Abegg, B., Pons, M., & Aall, C. (2019). A critical review of climate change risk for ski tourism. *Current Issues in Tourism*, *22*, 1343–1379. doi: https://doi.org/10.1080/13683500.2017.1410110
Sulser, T., Wiebe, K. D., Dunston, S., Cenacchi, N., Nin-Pratt, A., Mason-D'Croz, D., ... Rosegrant, M. W. (2021). *Climate change and hunger: Estimating costs of adaptation in the agrifood system*. Intl Food Policy Res Inst.
The World Bank. (2024). *World Development Indicators.* (`https://databank.worldbank.org/reports.aspx?source=2country=series=AG.LND.TOTL.K2period=` accessed 2024-06-06)
Tol, R. (2002a). Estimates of the damage costs of climate change. Part 1: Benchmark estimates. *Environmental and resource Economics*, *21*(1), 47–73. doi: https://doi.org/10.1023/A:1014500930521
Tol, R. (2002b). Estimates of the damage costs of climate change, Part II. Dynamic estimates. *Environmental and resource Economics*, *21*(2), 135–160. doi: https://doi.org/10.1023/A:1014539414591
Tol, R. S. (2014). Correction and update: The economic effects of climate change. *Journal of Economic Perspectives*, *28*(2), 221–226. doi: https://doi.org/10.1257/jep.28.2.221
Tol, R. S. J. (2009). The economic effects of climate change. *Journal of economic perspectives*, *23*(2), 29–51. doi: https://doi.org10.1257/jep.23.2.29
Toloo, G., FitzGerald, G., Aitken, P., Verrall, K., & Tong, S. (2013). Are heat warning systems effective? *Environmental health*, *12*(1), 27. doi: https://doi.org/10.1186/1476-069X-12-27
United Nations Environment Programme. (2023). Adaptation Gap Report 2023: Underfinance. Underprepared. Inadequate investment and planning on climate adaptation leaves world exposed. In (chap. Adaptation Finance Gap Update 2023). Nairobi: United Nations Environment Programme Publishing.
United Nations Environment Programme. (2025a). *Online annexes* (Tech. Rep.). Nairobi: United Nations Environment Programme Publishing. `https://wedocs.unep.org/20.500.11822/48798`.
United Nations Environment Programme. (2025b). *United Nations Environment Programme (2025). Adaptation Gap Report 2025: Running on empty. The world is gearing up for climate resilience — without the money to get there* (Tech. Rep.). Nairobi: United Nations Environment Programme Publishing. `https://wedocs.unep.org/20.500.11822/48798`.
Van Der Wijst, K.-I., Bosello, F., Dasgupta, S., Drouet, L., Emmerling, J., Hof, A., ... others (2023). New damage curves and multimodel analysis suggest lower optimal temperature. *Nature Climate Change*, *13*(5), 434–441. doi: https://doi.org/10.1038/s41558-023-01636-1
Van Vuuren, D. P., Edmonds, J., Kainuma, M., Riahi, K., Thomson, A., Hibbard, K., ... others (2011). The representative concentration pathways: an overview. *Climatic change*, *109*(1), 5. doi: https://doi.org/10.1007/s10584-011-0148-z

Walker, C. L. F., Friberg, I. K., Binkin, N., Young, M., Walker, N., Fontaine, O., … Black, R. E. (2011). Scaling up diarrhea prevention and treatment interventions: a lives saved tool analysis. *PLoS medicine*, *8*(3), e1000428. doi: https://doi.org/10.1371/journal.pmed.1000428

Ward, P. J., Winsemius, H. C., Kuzma, S., Bierkens, M. F. P., Bouwman, A., de Moel, A., … Luo, T. (2020). *Aqueduct Floods Methodology* (Tech. Rep.). World Resources Institute. `https://www.wri.org/research/aqueduct-floods-methodology`.

Wenz, L., Levermann, A., & Auffhammer, M. (2017). North-south polarization of European electricity consumption under future warming. *Proceedings of the National Academy of Sciences*, *114*, E7910-E7918. doi: https://doi.org/10.1073/pnas.1704339114

Winsemius, H., Van Beek, L., Jongman, B., Ward, P., & Bouwman, A. (2013). A framework for global river flood risk assessments. *Hydrology and Earth System Sciences*, *17*(5), 1871–1892. doi: https://doi.org/10.5194/hess-17-1871-2013.

Winsemius, H. C., Aerts, J. C. J. H., van Beek, L. P. H., Bierkens, M. F. P., Bouwman, A., Jongman, B., … Ward, P. J. (2016). Global drivers of future river flood risk. *Nature Climate Change*, *6*, 381–385. doi: https://www.doi.org/10.1038/NCLIMATE2893

Wong, P., Losada, I., Gattuso, J. P., Hinkel, J., Khattabi, A., McInnes, K., … Sallengar, A. (2014). Climate change 2014: Impacts, adaptation, and vulnerability. part a: Global and sectoral aspects. contribution of working group ii to the fifth assessment report of the intergovernmental panel on climate change. In (pp. 361–409). Cambridge: Cambridge University Press.

World Health Organisation. (2014). *Quantitative risk assessment of the effects of climate change on selected causes of death, 2030s and 2050s* (Tech. Rep.). Geneva: World Health Organisation Publishing.

World Health Organisation. (2020). *WHO Guidance for climate-resilient and environmentally sustainable health care facilities* (Tech. Rep.). World Health Organisation Publishing. https://www.who.int/publications/i/item/9789240012226.

World Health Organisation. (2021). *Global Technical Strategy for Malaria 2016-2030* (Tech. Rep.). World Health Organisation Publishing. https://iris.who.int/server/api/core/bitstreams/07fca8cd-f4ac-494a-9c30-b6b1dc499e07/content.

World Resources Institute. (2020). *Aqueduct floods.* (`https://www.wri.org/applications/aqueduct/floods//risk?p=eyJjb21tb24iOnsiZ2VvZ3VuaXRfdW5` 2024-05-05)

Yu, G., Schwartz, & Walsh, J. E. (2009). A weather-resolving index for assessing the impact of climate change on tourism related climate resources. *Climatic Change*, *95*, 551–573. doi: https://www.doi.org/10.1007/s10584-009-9565-7

Appendix A Regional composition

This paper calculates the gross damages, residual damages, adaptation costs and adaptation benefits for fifteen regions. The country composition of each region is shown using ISO codes in Table A.5.

Table A.5: **AD-MERGE 2.0 regional mapping**

Region	Code	Constituent countries (ISO-3)
Africa	AFR	AGO, BEN, BFA, BDI, BWA, CAF, CMR, COD, COG, COM, CPV, CIV, TCD, DJI, DZA, EGY, GNQ, ERI, ETH, GAB, GHA, GIN, GMB, GNB, KEN, LBR, LBY, LSO, MDG, MWI, MLI, MAR, MRT, MUS, MOZ, NAM, NER, NGA, RWA, STP, SEN, SYC, SLE, SOM, SSD, ZAF, SDN, SWZ, TZA, TGO, TUN, UGA, ZMB, ZWE
Australia and New Zealand	ANZ	AUS, NZL
Brazil	BRA	BRA
Canada	CAN	CAN
China	CHN	CHN
India	IND	IND
Japan and South Korea	JSK	JPN, KOR
Mexico	MEX	MEX
Middle East	MEA	BHR, IRN, IRQ, ISR, JOR, KWT, LBN, OMN, PSE, QAT, SAU, SYR, ARE, YEM
Other Asia	OAS	AFG, BGD, BTN, MMR, BRN, KHM, CHN, HKG, IND, IDN, LAO, MAC, MYS, MDV, MNG, NPL, PRK, PAK, PHL, PNG, SGP, LKA, TLS, THA, VNM; Oceania (excluding Australia and New Zealand): ASM, COK, FJI, PYF, GUM, KIR, MHL, FSM, NRU, NIU, MNP, PLW, PNG, WSM, SLB, TKL, TON, TUV, VUT, WLF
Other Central and South America	CLA	ARG, BOL, CHL, COL, ECU, FLK, GUY, PRY, PER, SUR, URY, VEN, BLZ, CRI, SLV, GTM, HND, NIC, PAN, AIA, ATG, ABW, BHS, BRB, BMU, BES, VGB, CYM, CUB, CUW, DMA, DOM, GRD, GLP, HTI, JAM, MTQ, MSR, PRI, BLM, KNA, LCA, MAF, VCT, TTO, TCA, VIR
Other Eurasia	OEA	ALB, ARM, AZE, BLR, BIH, BGR, CYP, GEO, KAZ, KGZ, LVA, LTU, MDA, MKD, ROU, SRB, TJK, TUR, TKM, UKR, UZB
Russia	RUS	RUS
United States of America	USA	USA
Western Europe	WEU	AND, AUT, BEL, CHE, CZE, DEU, DNK, EST, FIN, FRA, FRO, GBR, GIB, GRC, GRL, HRV, HUN, IRL, ISL, ITA, LIE, LUX, MCO, MLT, MNE, NLD, NOR, POL, PRT, SMR, SVK, SVN, SWE, VAT

Note: Country codes are ISO-3.